JOURNAL OF OPTOELECTRONICS AND ADVANCED MATERIALS, Vol. 12, No. 6, June 2010, p. 1385 - 1393

Interlayer magnetic coupling in exchange bias and spin valve structures with Fe-Mn and Ir-Mn antiferromagnetic layers

V. KUNCSER, W. KEUNE[a], U. von HÖRSTEN[a], G. SCHINTEIE
National Institute of Materials Physics, P.O. Box MG 7, 77125, Bucharest-Magurele, Romania
[a]Fakultät fürPhysik, Universität Duisburg-Essen (Campus Duisburg), D-47048 Duisburg, Germany

Exchange bias AF/Fe and spin valve AF/Fe/Cu/Fe (AF=$Fe_{50}Mn_{50}$ and $Ir_{50}Mn_{50}$) multilayer systems have been prepared by molecular beam epitaxy. Thin tracer layers enriched in the ^{57}Fe isotope were artificially grown at the AF/Fe interface and the phase composition of the ferromagnetic layer, as well as the interfacial atomic diffusion were observed via ^{57}Fe conversion electron Mössbauer spectroscopy. The dependence of the magnetization reversal process on training and temperature associated effects was studied by low temperature vibrating sample magnetometry, whereas the interlayer magnetic coupling was analyzed via longitudinal magneto-optic Kerr effect.

(Received March 28, 2010; after refvision May 10, 2010; accepted June 16, 2010)

Keywords: Interfacial magnetic coupling, Multilayers, Mössbauer effect, Magneto-optic Kerr effect, Magnetometry

1. Introduction

The hysteresis loop of a ferromagnetic layer which is interfacially coupled to an antiferromagnetic layer is drastically modified with respect to the one of a similar free ferromagnetic layer. In general, it shows a larger coercive field and in particular cases it may present also a shift from the zero field. The shift (mainly negative) is known as an exchange bias field and is related to a so-called unidirectional anisotropy [1]. Both these characteristics of the exchange coupled ferromagnetic layers can be used in magnetic devices where the electron conduction is manipulated via Giant Magneto-Resistance (GMR) effects [2-4]. The main element of such a device could be in principle a multilayer structure of type AF/F1/Cu/F2, with AF, an antiferromagnetic layer, F1 and F2 an interfacially coupled and a free ferromagnetic layer, respectively, and Cu, a conductive layer, all of nanometer thickness. According to the GMR effect in layered systems, the electron transport through the Cu conductive thin layer is controlled via the relative orientation of the spins (or magnetizations) in the adjacent ferromagnetic layers. The switching from the parallel to the antiparallel magnetic configuration of the two ferromagnetic (F) layers might be realized via the application of suitable magnetic fields, within the condition to have distinct hysteresis loops for the two layers. If the two layers F1 and F2 are not coupled to each other, the complex loop of the above mentioned spin valve structure can be decomposed into the shifted hysteresis loop of the F layer exchange coupled to the AF layer and the loop of the free F layer which is centered on zero field. In the ideal case of ferromagnetic layers of negligible coercivity, the overall spin orientation in the two F layers during the magnetization reversal can be similar or opposite, depending on the value of the applied field with respect to the exchange bias field. The exchange bias field, H_E, as one of the crucial parameters of a spin valve structure, may be roughly expressed via the relationship $H_E=\sigma/M_r t$, where σ is the interfacial exchange energy, M_r the remanent magnetization of the pinned F layer and t its thickness [1,2,5]. Evidently, both the interfacial exchange energy and the remanent magnetization depend on many other variables such as the type of the F films, their crystalline structure and phase composition, the quality of the AF/F interface, etc. [6-8]. In addition, the interfacial exchange energy (and hence, the exchange bias field) decreases with increasing temperature, due to specific magnetic relaxation mechanisms. The blocking temperature, T_B, defined as the temperature where the exchange bias field decreases to zero [2,6,9], depends on the type and characteristics of the AF film. One of the most convenient AF materials serving as pinning layer in giant magneto resistive elements, with respect to both the interfacial exchange energy and the blocking temperature, is the equiatomic Fe-Mn alloy. Bulk Fe-Mn disordered alloys present the fcc structure (lattice parameter of about 0.36 nm) and antiferromagnetic ordering at room temperature, for Fe concentrations ranging from 45 at. % to 75 at. % [10,11]. The Néel temperature reaches a maximum of about 500 K for 50 at. % Fe. Even under these conditions, the blocking temperature for exchange bias is only slightly above 370 K, for well crystallized films with a thickness higher than

the critical one (25 nm). Due to these properties, the $Fe_{50}Mn_{50}$ alloy has become the most utilized AF material in spin valves for more than one decade. Presently it has been replaced by Ir-Mn alloys which show a higher corrosion resistance, a more convenient blocking temperature (about 550 K for 20 at. % Ir) and a lower critical thickness (about 8 nm) [5]. However, all the above mentioned parameters depend drastically on the structure and morphology of the AF layer and on the quality of the AF/F interface. The present paper deals with a study of the magnetic properties of multilayers of type AF/F and AF/F/Cu/F (F=Fe and AF = either $Fe_{50}Mn_{50}$ or $Ir_{50}Mn_{50}$) by low temperature vibrating sample magnetometry (VSM) and room temperature magneto-optic Kerr effect (MOKE). The phase composition of the ferromagnetic layer as well as the quality of the AF/F interface were also studied by ^{57}Fe conversion electrons Mössbauer spectroscopy (CEMS).

2. Experimental

The layered structures were grown by molecular beam epitaxy (MBE) on commercial Si substrates. Firstly, a Cu buffer layer (15 nm thick) was grown at 100°C, and subsequently the AF thin films (15 nm thick) were deposited (also at 100 °C) by co-evaporation from two sources at a pressure of $8 \cdot 10^{-10}$ mbar during deposition. Fe or Fe/Cu/Fe layers were finally grown at the same temperature and protected by a 5 nm thick Cu cap layer. The evaporation rates were monitored with calibrated quartz-crystal microbalances. In the case of the AF films the rates correspond to the equiatomic composition of Fe-Mn or Ir-Mn. Tracer layers of ^{57}Fe (1.5 nm thick) were deposited at the F/AF interface. The four different samples considered for this study correspond to the following geometrical structure (see also figure 1 with AF=Fe-Mn or Ir-Mn):

Sample FeMn_01: Si/Cu(15nm)/$Fe_{50}Mn_{50}$(15nm)/^{57}Fe(1.5nm)/^{nat}Fe(3.5nm)/Cu(5nm)
Sample FeMn_03: Si/Cu(15nm)/$Fe_{50}Mn_{50}$(15nm)/^{57}Fe(1.5nm)/ ^{nat}Fe(3.5nm) /Cu(5nm)/ ^{nat}Fe(5nm)/Cu(5nm)
Sample IrMn_01: Si/Cu(15nm)/$Ir_{50}Mn_{50}$(15nm)/^{57}Fe(1.5nm)/^{nat}Fe(3.5nm)/Cu(5nm)
Sample IrMn_03: Si/Cu(15nm)/$Ir_{50}Mn_{50}$(15nm)/^{57}Fe(1.5nm)/ ^{nat}Fe(3.5nm)/ Cu(5nm)/ ^{nat}Fe(5nm)/Cu(5nm)

In the above notation, ^{nat}Fe labels a metallic layer grown from natural Fe (mainly ^{56}Fe and only ~ 2% natural abundance of ^{57}Fe), whereas ^{57}Fe labels a metallic layer grown from Fe enriched to 95% in the ^{57}Fe isotope. It is worth mentioning that the crystalline structure and electronic properties of the ^{57}Fe layer are identical to the ^{nat}Fe layer (body centered cubic, bcc), the only difference consisting in the enhanced sensitivity of the tracer layer (47 times higher than for a non-enriched layer of the same thickness) with respect to ^{57}Fe Mössbauer spectroscopy. From the magnetic point of view, sample FeMn_01 is an exchange bias AF(15nm)/F(5nm) bilayer, whereas sample FeMn_03, is a spin valve structure of type AF(15nm)/F(5nm)/Cu(5nm)/F(5nm). The second set of two samples is similar to the set just described, the only difference being the use of IrMn instead of FeMn for the AF layer. The Cu buffer layer exhibits the face centred cubic (fcc) structure for both $Fe_{50}Mn_{50}$ and $Ir_{50}Mn_{50}$ films, as proven by preliminary X-ray diffraction measurements. None of the typical procedures for inducing the exchange bias effect in the F layer coupled to the AF layer (field cooling from above the Néel temperature of the AF phase or an applied field during the growing process) were applied. However, low temperature magnetometry was performed after cooling the sample from room temperature (which is lower than the Néel temperature of either Fe-Mn or Ir-Mn AF phases) down to the measurement temperature, in a magnetic field higher than the saturation field of the F layer.

The phase composition and local magnetic interactions within the F layer as well as the atomic interdiffusion processes at the interface with the AF layer were investigated by ^{57}Fe CEMS.

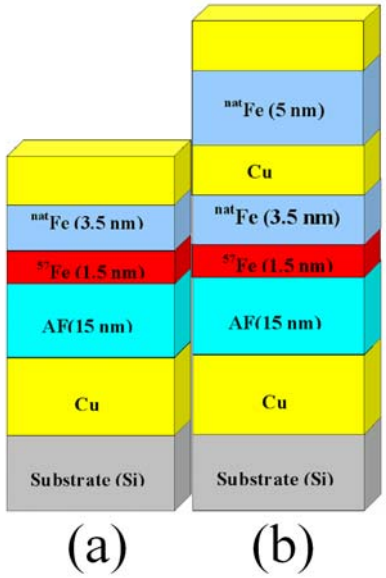

Fig. 1. The geometrical structure of the analyzed systems, namely: AF_01 (a) and AF_03 (b). AF can be either FeMn or IrMn. ^{57}Fe tracer layers were artificially grown at the AF/F interfaces.

The CEMS measurements were performed at room temperature with a constant acceleration spectrometer and a gas-flow proportional counter using a He-CH_4 mixture. A ^{57}Co-source in a Rh-matrix was used. All spectra were recorded in perpendicular back-scattering geometry, i.e. with the incident γ-ray direction perpendicular to the multilayer plane. The CEMS spectra were fitted using the "NORMOS" package developed by Brand [12]. All isomer shifts (IS) are given relative to bulk α-Fe at room

temperature (RT). The global magnetic properties of the multilayers were studied at room temperature (RT) by longitudinal MOKE (magneto-optic Kerr effect using laser light of 680 nm) and at low temperature by VSM (vibrating sample magnetometry). A MOKE device working in longitudinal geometry and using a magnet with laminated sheets with essentially zero remanence and negligible hysteresis, was employed. The low temperature hysteresis loops were obtained by a closed cycle (Cryogenics) vibrating sample magnetometer working down to 1.8 K, in applied fields of up to 9 T and with a sensitivity of 10^{-5} emu. The magnetic field was applied along the sample plane.

3. Results and discussion

The ^{57}Fe Mössbauer spectra obtained at RT on FeMn and IrMn exchange bias bilayers with ^{57}Fe tracer layers placed at the F/AF interface are shown in figure 2. The best fitting was achieved by using three Mössbauer components with Lorentzian line shape: (i) a most intense sharp outer Zeeman sextet (S_1), (ii) a less intense inner Zeeman sextet (S_2), and (iii) a relatively broad central paramagnetic pattern (CP). The spectral parameters of the Mössbauer components of each sample, obtained from least-squares fitting, are presented in Table 1. Based on the values of its hyperfine parameters (see Table 1), the outer sextet is assigned to the ^{57}Fe-layer region away from the interface and will be considered in the following as belonging to a bulk-like Fe layer which is not influenced by interfacial atomic diffusion.

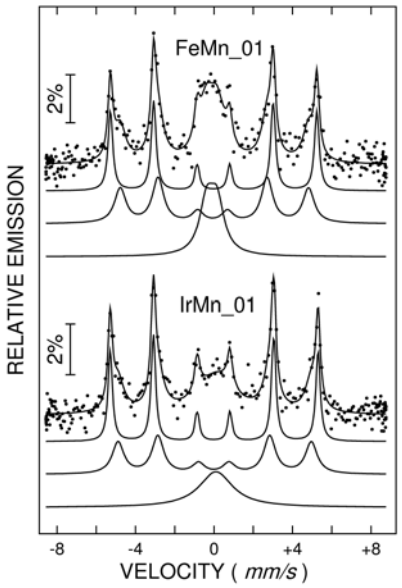

Fig. 2. Room temperature conversion electrons Mössbauer spectra of exchange bias structures FeMn_01 and and IrMn_01 with a 1.5 nm tracer layer of ^{57}Fe at the F/AF interface.

The inner sextet with a magnetic hyperfine field lower than 30.1 T is due to a defective bcc Fe phase in the direct and close neighbourhood of the AF/F interfaces and will be considered as sensing the interfacial atomic diffusion of the low size Mn atoms from the antiferromagnetic layer into the ^{57}Fe probe layer. Because the corresponding hyperfine field of S2 is lower in FeMn_01 than in IrMn_01 (29.6 T as compared to 30.1 T, respectively), this suggests a slightly higher Mn concentration at the F/AF interface in FeMn as compared to IrMn systems. The relative spectral area of the outer sextet (S1) is slightly larger than that of the inner sextet (S2) in IrMn based systems, but they are almost equal in the FeMn systems. Having in mind the overall thickness of the ^{57}Fe tracer layer (1.5 nm), a crude estimation, starting from the relative areas of the two sextets, leads to a defective ^{57}Fe interface region of about 0.6 nm thickness in IrMn bilayer and a slightly thicker interface region (about 10% larger) in the FeMn bilayer. The rest of the about 4.4 nm thick layer of Fe presents a well crystallized bcc-like structure, for which magnetic parameters close to the ones specific to bulk Fe can be expected. However, the slightly sharper F/AF interface in the IrMn systems as compared to the FeMn based systems, can not explain the large difference in their magnetic properties, which will be presented in the following. Therefore, these properties have to originate rather from the different magnetic properties of the AF layer, with influence on the exchange coupling effects.

The central paramagnetic pattern (CP), fitted either as a broad singlet or as an unresolved quadrupole doublet, is attributed to the diffusion of the ^{57}Fe atoms into the AF layer and is beyond our interest, due to the relatively low contribution to the Mössbauer spectra (the increased contribution in the Fe/FeMn system is due to the additional CP-signal coming from the Fe atoms in the thick FeMn antiferromagnetic layer). The linewidth of the inner sextet as well as of the paramagnetic pattern is relatively large, as expected from the strong interfacial diffusion manifesting in these very interfacial alloy phases.

From the magnetic point of view, further useful information obtained from the Mössbauer spectra is related to the ratio between the intensity of the second and the third spectral line, denoted as R_{23}, of the sextets S1 and S2. For both sextets and for all samples, the R_{23} value was found to be 3.7(1), i.e., very close to the maximum value of 4, specific to a full in plane orientation of the Fe spins in the ferromagnetic layer. Therefore, due to this in plane shape anisotropy, the magnetization reversal processes were followed with the magnetic field applied within the sample plane.

Table 1. Relative area of spectral components (S1=outer sextet; S2=inner sextet; CP=central pattern), magnetic hyperfine field (B_{hf}), isomer shift (IS), quadrupole nuclear level shift ε (=QS/2) and linewidth (w), as obtained from the Mössbauer spectra.

Sample	Spectral component	Rel. area (%)	Hyperfine magnetic field (T)	Isomer shift (mm/s)	Quadrupole shift (mm/s)	Linewidth (mm/s)
FeMn_01	S1	37(1)	32.5	-0.01	0.00	0.30
	S2	37(2)	29.6	-0.01	0.00	0.70
	CP	26(2)	-	-0.11	0.26	0.85
IrMn_01	S1	44(1)	32.8	0.01	0.01	0.28
	S2	41(1)	30.1	0.02	0.03	0.80
	CP	15(1)	-	+0.12	0.00	0.80

The hysteresis loop obtained at 5 K by VSM, after field cooling the spin valve structure FeMn_3 from RT in an applied field of 0.2 T, is shown in figure 3. The loop exhibits a complex and asymmetrical shape and is shifted in average towards a negative field. In fact, taking into account the geometrical structure of the analysed multilayer, one has to consider that the experimentally obtained overall loop is the result of a superposition of two different loops, one of higher coercivity, shifted by the exchange bias field and belonging to the bottom F layer that is pinned to the AF film, and a second one of lower coercivity and almost centered at zero field, belonging to the free F top layer. When the two loops are well distinguishable (e.g. for high exchange bias field and low coercivity of the pinned layer), there is no difficulty for retrieving the entire information concerning the magnetic reversal process in each layer. In the present case, where these conditions are not fulfilled, the information is not any more transparent and a careful analysis of the loops is required.

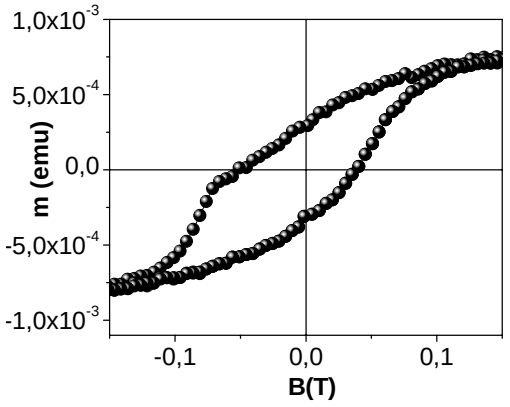

Fig. 3. First hysteresis loop obtained at 5 K after field-cooling sample FeMn_03 in a magnetic field of 0.2 T.

Before discussing a newly proposed procedure for estimating exchange bias effects in such complex cases, it is worth to mention the physical reason leading to this situation. Because of the broad X-ray diffraction lines observed for these systems (with the main contribution coming from the thick AF layer), it is consequential to consider very small crystallites in the AF film. Therefore, each AF crystallite will show a low number of spins, N, at the interface with the ferromagnetic layer. According to the magnetic relaxation model of exchange bias by Stiles and McMichael [13], for a given domain wall energy at 0 K, σ_0, the exchange bias field decreases when the average interfacial coupling energy, NJ_{net}, is decreasing ($NJ_{net}=J_{int}/(N_1-N_2)/$ with J_{int} the interfacial exchange coupling constant and $/(N_1-N_2)/$, the absolute value of uncompensated spins at the interface). Evidently, NJ_{net} in the present system is low in the average, firstly because N is low and secondly, because the field-cooling process started from below the Néel temperature of the AF phase (therefore, uncompensated spins are induced mainly in the finest AF grains). If a size distribution is considered for the AF grains (leading to a distribution of interfacial coupling energies), a distribution of low exchange bias fields for different domains of the ferromagnetic layers may be supposed, which might be in fact the origin of the very broad hysteresis observed at 5 K.

In order to clarify some general aspects related to the observed complex hysteresis loop, a superposition of two hypothetical hysteresis loops of similar saturation magnetization (as imposed by identical F layers with the same thickness) is shown in figure 4(a). The two simulated components (presented in the inset on the left side of figure 4(a)) correspond to the following parameters given in arbitrary units (a.u.): 5 a.u. saturation magnetization, 6 a.u. coercive field and -2 a.u. exchange bias field for the pinned F layer, and 5 a.u. saturation magnetization, 2 a.u. coercive field and 0 a.u. exchange bias field for the free F layer. Two aspects have to be mentioned for the simulated overall loop: (i) it has no centre of symmetry and (ii) the enclosed area under the loop at positive fields is different from the one at negative fields. Both of these characteristics, observed also in the experimental overall loop, can be considered as signatures for the presence of the exchange bias field in the pinned F layer.

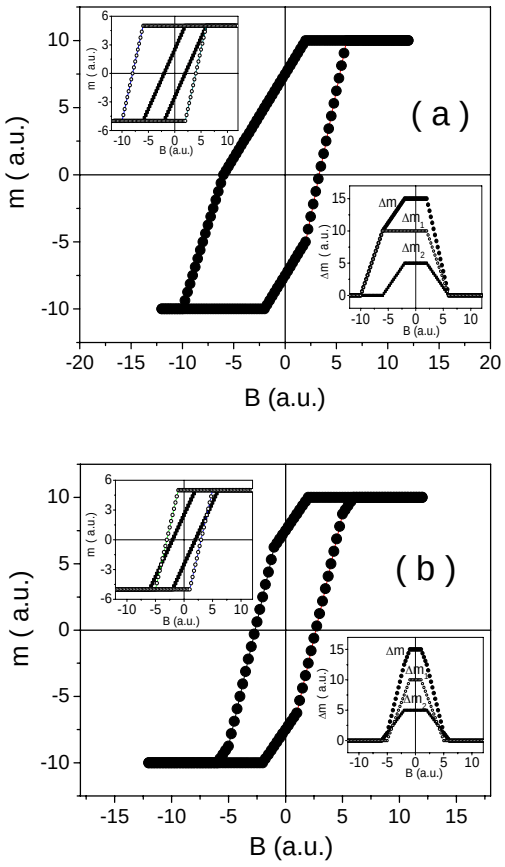

Fig. 4. Simulation of hysteresis loops generated by different couples of two non-interacting ferro-magnetic layers, with different anisotropies. The hypothetical loops, corresponding to each layer, with parameters given in the text, are shown in the insets on the left side. In the first case, (a), one layer presents both unidirectional (exchange bias) and uniaxial anisotropy and the other one only uniaxial anisotropy. In the second case, (b), both layers present only uniaxial anisotropy. The differences, Δm, and their components, Δm_1 and Δm_2, defined in the text, are shown in the inset on the right side.

However, starting from the overall loop, estimations concerning the magnitude of the exchange bias fields or of coercive fields of the two components are not available due to the real difficulties in its proper decomposition in the two components. A more convenient procedure for an estimation of the exchange bias field would be to form up the difference $\Delta m = m_u - m_l$, where m_u is the upper branch of the overall loop and m_l is its lower branch, versus the applied field. This curve is presented in the inset on the right side of figure 4(a). Obviously, Δm can be decomposed as follows: $\Delta m = \Delta m_1 + \Delta m_2$, where Δm_1 and Δm_2 are equal to the magnetization difference of the two (upper and lower) branches, belonging to the pinned and the free F layers, respectively. The two components Δm_1 and Δm_2 are shown in the same inset. Clearly, the difference Δm versus the applied field provides similar signatures as the overall loop, regarding the presence of the exchange bias field, via the following characteristics: (i) there is no reflection symmetry axis of the dependence Δm(B), and (ii) the comprised area under the dependence Δm(B) at positive fields is different from the one at negative fields.

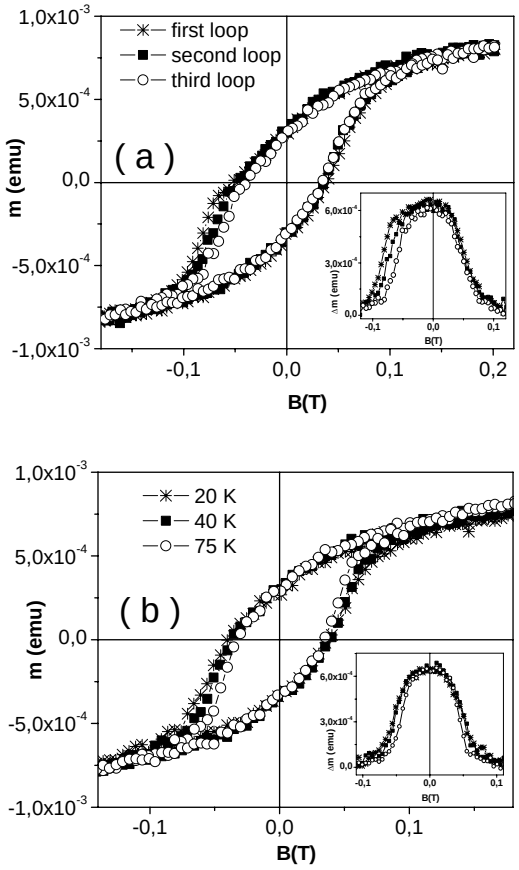

Fig.5. Three consecutive hysteresis loops of sample FeMn_03 field-cooled to 5 K in 0.2 T applied field (a) and hysteresis loops obtained at three increasing temperatures (b). The differences Δm, defined in the text, are shown in the insets.

However, at least a rough decomposition of the dependence Δm(B) in the two components Δm_1 and Δm_2 as well as an evaluation of the exchange bias field can be provided in some limiting cases. For example, the most usual assumption for overlapped loops (often supported by the considered spin valve structures with polycrystalline layers) is that Δm_1 (for the pinned F layer) and Δm_2 (for the free F layer) start to increase at the same positive field, whereas Δm_1 decreases to zero at the most negative field (due to the higher coercive field of the pinned layer). That is, the exchange bias field, which is related to the variation of Δm_1, can be suitably estimated as an average of the two field values (positive and negative), where the overall

Δm(B) approaches zero. Indeed, in the presented simulation, these fields correspond to 6 a.u and -10 a.u., respectively, leading to the initially considered exchange bias field of -2 a.u. for the pinned layer.

The second hypothetical case, which is going to be considered, concerns two hysteresis loops corresponding to a free F layer and a similar F layer pinned to the AF film by only uniaxial anisotropy (the unidirectional anisotropy leading to the exchange bias effect is neglected). The following parameters of the component loops were considered: 5 a.u. saturation magnetization, 3 a.u. coercive field and 0 a.u. exchange bias field for the pinned F layer, and 5 a.u. saturation magnetization, 2 a.u. coercive field and 0 a.u. exchange bias field for the free F layer. The overall loop is shown in figure 4(b), and the two components are presented in the inset on the left side of the figure. The particular aspect of this representation, namely the symmetry centre of the overall loop at zero field, is the signature for the lack of the exchange bias in the pinned F layer. Similarly, the difference Δm(B) and its components $\Delta m_1(B)$ and $\Delta m_2(B)$ are shown in the inset at the right side of the figure. All these dependences are symmetrical with respect to the zero field axis, as expected for the lack of any kind of unidirectional anisotropy.

The evolution of the exchange bias field and of the interlayer magnetic couplings in the analyzed systems, during training and temperature variation effects, will be further discussed in terms of the previous observations.

The first three consecutive loops obtained after field-cooling sample FeMn_03 to 5 K in 0.2 T are shown in figure 5(a) (the fourth successive loop is almost superimposing with the third loop) whereas the corresponding differences Δm(B) are presented in the inset. It can be observed that the lower part of the upper branch is slightly shifted towards the right and the complex shape becomes more symmetrical after successive magnetic reversals. The exchange bias field assigned to the F pinned layer is decreasing, reaching a stationary value already at the third cycle. The estimations of the exchange bias field which were obtained from the Δm(B) curves by the above described approach are: H_E=-120 Oe, -60 Oe and -40 Oe for the first, second and third loop, respectively. After reaching the saturation produced by the training effect, subsequent loops were obtained at increasing temperatures, in order to evaluate the blocking temperature (T_B) for exchange bias. Three hysteresis loops (and the corresponding Δm(B) curves) are shown in figure 5(b). An exchange bias field of -30 Oe was estimated at 20 K. At 40K and 75 K the bias field becomes negligible (in the limit of experimental errors) and the shrinkage of the hysteresis loop, symmetrically towards the branching points, has to be related only to a decrease of the coercivity in the pinned F layer at higher temperatures.

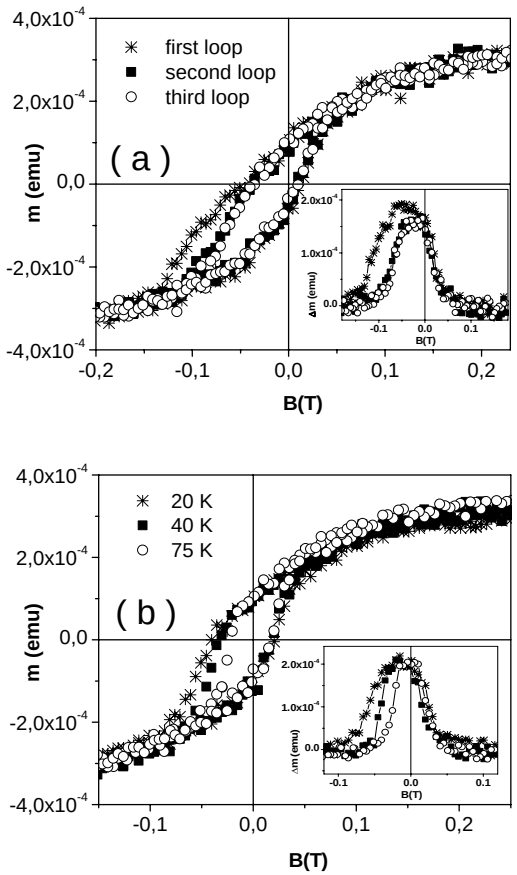

Fig.6. Three consecutive hysteresis loops of sample IrMn_03 field-cooled to 5 K in 0.2 T applied field (a) and hysteresis loops obtained at three increasing temperatures (b). The differences Δm, defined in the text, are shown in the insets.

Similar data were also obtained for the IrMn_03 sample. The first three consecutive hysteresis loops obtained after field-cooling the sample to 5 K in a field of 0.2 T are shown in figure 6(a) (training effects), and three hysteresis loops obtained at increasing temperatures after reaching the training saturation are shown in figure 6(b) (Δm(B) data are presented in the inset of each figure). The estimated exchange bias field at 5 K is substantially higher than in the case of the FeMn based sample, namely about -500 Oe for the first cycle and -330 Oe for the second and the third cycle. Evidently, the bias field reaches the saturation by training effects already after the second cycle and subsequent cycles taken after the third one, at increasing temperatures, give information restricted only to the blocking temperature. By using data from figure 6(b), exchange bias fields of -200 Oe, -90 Oe and almost 0 Oe were obtained at 20K, 40 K and 75 K, respectively. It is worth mentioning at this point that neither the complex hysteresis loops nor the Δm(B) curves can be suitable handled in order to get reliable values for the coercive fields of the two F layers. Above the blocking temperature (about 40 K in the case of FeMn samples and 75 K for IrMn samples, respectively), the unidirectional

anisotropy in the pinned layer is already zero, but no information about the relationship between the two coercive forces in the pinned and the free F layer is available (if they are equal or not, an overall symmetrical loop centred at zero field is obtained).

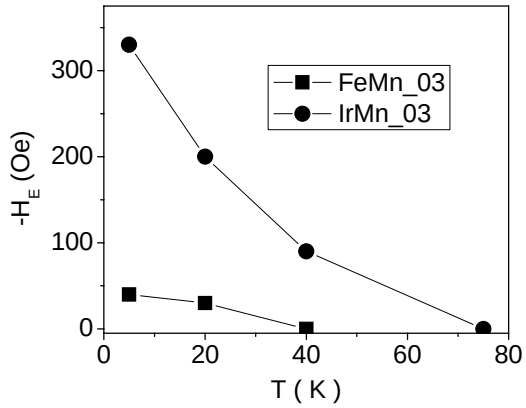

Fig. 7. Saturated exchange bias field versus temperature for FeMn_03 and IrMn_03 structures. The effect was partially induced by cooling the sample in an applied field from room temperature only.

The dependences of the saturation exchange bias field (after removing training effects at low temperature) versus temperature, for both FeMn_03 and IrMn_03 samples, are shown in Figure 7. As observed, the exchange bias field in the static regime (at 5 K) is almost eight times higher in the IrMn based sample than in the FeMn one (e.g. it is 330 Oe in IrMn sample as compared with only 40 Oe in FeMn sample), whereas the blocking temperature of the former is almost twice the one of the second. However, both the observed exchange bias fields and the blocking temperatures are many times lower than the usually reported ones for such system [2,5]. There are two reasons which might be responsible for such a behaviour in our analysed samples: (i) the low crystallite average size of the AF layer and (ii) the field cooling process which in our case was performed from room temperature (which is lower than the Néel temperature of well crystallized AF phases involved in the systems).

Concerning the first issue, it is reported that the unidirectional anisotropy (and hence, the exchange bias field) is dependent on the preparation conditions of the AF layer, in similar geometrical structures [14]. Hence, the substrate temperature of only 100˚C during the deposition of the AF layer could be a sensible reason for its low size crystallites. Secondly, very fine AF crystallites could be either very defected (e.g. presenting a lower Néel temperature as compared to the bulk value) or could show a superparamagnetic behaviour at room temperature, as reported by Anhoj et al. [15]. In either of the two cases, only such small crystallites with a relatively low magnetic transition temperature could become effective in inducing exchange bias effects, when the system is cooled down in applied magnetic field from room temperature.

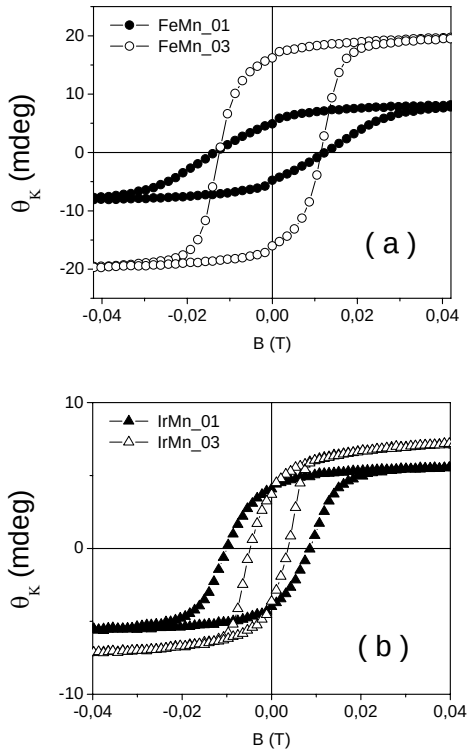

Fig.8. Longitudinal MOKE loops of exchange bias and spin valve structures with FeMn (a) and IrMn (b) antiferromagnetic layers

Therefore, in case of size distributed crystallites in the AF phase, due to the applied field cooling procedure, only a small fraction of them are effective in inducing the unidirectional anisotropy. While this fraction corresponds to the lowest sizes, relatively low exchange bias fields and blocking temperatures are expected. Finally, a last aspect concerns the second derivative of the two temperature dependences in Fig.7. The exchange bias field increases sharply upon cooling at low temperature in case of the IrMn_03 sample, but reaches a certain saturation in case of the FeMn_03 sample and, hence, the second derivative is positive in the first case and negative in the second. The two different trends can be explained again in the frame of the relaxtion model by Stiles and McMichael [13] in terms of the ratio between the interfacial coupling energy and the domain wall energy in the AF grains. Clearly, the sharper increase of the unidirectional anisotropy at low temperature involves an interfacial coupling energy approaching the domain wall energy in case of the IrMn_03 samples. On the other hand, the saturating trend observed in case of the FeMn_03 sample supports an interfacial coupling energy much lower than the wall energy in such systems. The wall energy is directly proportional to the square root of the uniaxial anisotropy constant of the AF phase, K_{AF} , which influences directly

the coercive field of the exchange coupled ferromagnetic layer. However, this coupled ferromagnetic layer gives rise to the largest opening (coercivity) of the complex hysteresis loops of the two systems at 5 K (figure 5b and figure 6b) which can be very roughly estimated at about 450 Oe and 300 Oe for FeMn and IrMn based systems, respectively. Accordingly, almost comparable wall energies can be supposed for the two systems. Hence, the two specific trends of the temperature evolution of the exchange bias fields are well supported by the more enhanced exchange bias field at 5 K (equivalently to a more enhanced unidirectional interfacial coupling) in IrMn systems as compared to the FeMn case.

Finally, a real interest in such systems is related to the strength of the coupling between the two ferromagnetic layers sandwiching the Cu conductive layer (5 nm thickness). In order to answer this question, MOKE loops have been taken on both the exchange bias and the spin valve structures. Due to the specific geometrical structure of the samples, a penetration depth of the light (He-Ne, λ=680 nm) down to ~~only the first~~ even the second F layer is expected (the second ~~one~~ layer is placed at about 15 nm below the stack surface in spin valve structures, if the cap layer is also considered). The MOKE loops obtained at RT on samples FeMn_01 (AF/F structure) and FeMn_03 (AF/F/Cu/F structure) are shown in figure 8(a), whereas the loops obtained on similar structures, but with IrMn AF films, IrMn_01 and IrMn_03, are depicted in figure 8(b). All the presented loops are symmetrical and non-shifted in field, proving the presence of only uniaxial anisotropy (reference loops obtained on F layers grown directly on Cu buffer layers show coercive fields lower than 20 Oe). One can observe that both loops corresponding to FeMn_01 and FeMn_03 samples reveal an identical coercive field of 120(3) Oe. While light may penetrates ~~only~~ in the ~~first~~ second ferromagnetic layer, the two loops correspond to the ferromagnetic pinned layer (in FeMn_01) and the free and pinned layer (in FeMn_03), respectively. Their identical coercivities show that the two layers reverse their magnetization in the field simultaneously, as they are magnetically coupled to each other. This effect is not unexpected, being already observed in spin valve systems [16]. It is due to the magnetostatic (or Néel, or orange-peel) coupling which is specific to rough interfaces with conformal sinusoidal-like morphologies [4,17]. Due to the small thickness of the layers involved in the F/Cu/F stacks, the magnetostatic coupling may overpass the magnitude of the AF/F exchange anisotropy, becoming harmful to a proper decoupling of the two ferromagnetic layers.

The loop of sample IrMn_03 shows a much lower coercivity than that of the sample IrMn_01 (only 44(3) Oe as compared with 90(3) Oe, respectively) and the magnitude of the MOKE signal is only slightly larger. That is, in the case of the IrMn_03 structure, the MOKE signal comes mainly from the top F layer which has a much lower uniaxial anisotropy as compared to the bottom pinned F layer and switches the magnetization independently.

4. Conclusions

Exchange-bias and spin-valve structures with $Fe_{50}Mn_{50}$ and $Ir_{50}Mn_{50}$ antiferromagnetic pinning layers and Cu conductive spacer layers located between the pinned and the free Fe ferromagnetic layers have been prepared by MBE. Tracer layers enriched in ^{57}Fe were placed at the F/AF interface in order to study the interfacial atomic diffusion and the real phase composition of the F layer. It was found that the ferromagnetic layer is well crystallized in the typical bcc bulk like Fe structure, except of an almost 10% interfacial thickness where the structure is perturbed by the diffusion of Mn atoms from the AF layer into the Fe layer. With respect to the atomic diffusion, the F/AF interface in IrMn systems is slightly sharper as compared to FeMn based ones.

Hysteresis loops obtained via vibrating sample magnetometry have evidenced a rapid saturation of the exchange bias field at 5 K by training effects and rather low blocking temperatures, with better results for systems with IrMn AF layers. A new methodological procedure for subtracting information on the exchange bias field from complex-shaped hysteresis loops with distributed parameters is proposed. The stationary exchange bias field at 5 K is almost eight times higher in the structure with IrMn AF films as compared to the structure with FeMn AF films. MOKE hysteresis loops acquired at room temperature provided a much weaker magnetostatic (orange peel) coupling between the ferromagnetic layers for systems with IrMn AF films.

All the results show that compared to FeMn based systems, the IrMn based ones present much improved magnetic characteristics with respect to requirements of spin valve structures. However, the prepared systems show lower exchange bias fields and blocking temperatures as compared to similar systems reported in literature, most probable due to specific preparation conditions and field cooling procedures.

Acknowledgements

The work at Bucharest was supported by the National Agency for Scientific Research, Project PNII-032/2007 and at Duisburg-Essen by the Deutsche Forschungsgemeinschaft (SFB 491).

References

[1] W. H. Meiklejohn, C. P. Bean, Phys. Rev. **102**, 1413 (1956).
[2] J. Nogues, I.K.Schuller J.Magn.Magn.Mater. **192**, 203 (1999).
[3] M. Johnson, Magnetoelectronics edited by Elsevier Amsterdam Cap 1 and 2 (2004).
[4] S. A Wolf , D. Treger, A. Chtchelkanova, MRS Bulletin **31**, 400 (2006).
[5] I. R. McFadyen , E. E. Fullerton, M. J. Carey, MRS Bulletin **31**, 379 (2006).

[6] F. Radu, H. Zabel, Exchange Bias Effect of Ferro-/Antiferromagnetic Heterostructures, Springer Tracts in Modern Physics **227**, 97 (2007).
[7] F. Stromberg , W. Keune , V. Kuncser, K. Westerholt, Phys.Rev. B **72**, 064440 (2005).
[8] V. Kuncser, M. Valeanu, G. Schinteie, I. Mustata , C. P. Lungu , A. Anghel , H. Chiriac , R. Vladoiu J. Bartolome, J. Magn. Magn. Mater. **320**, e226 (2008).
[9] C. Hou, H. Fujiwara, K. Zhang, A. Tanaka, Y. Shimizu, Phys.Rev B **63**, 024411 (2000) .
[10] Y. Endoh, Y. Ishikawa, J.Phys.Soc.Jpn **30**, 1614 (1971).
[11] F. Offi, W. Kuch, J. Kirschner, Phys.Rev. B **66**, 064419 (2002).
[12] R. A., Brand, Nucl. Instr. Meth. Phys. Res. B **28**, 398 (1987).
[13] M. D. Stiles, R. D. McMichael, Phys.Rev. B **60**, 12950(1999).
[14] K. Yogami , M. Tsunoda, M.Takahashi, J.Appl.Phys. **87**, 4930(2000).
[15] T. A. Anhoj, C. S. Jacobsen, S. Morup, J. Appl. Phys. **95**, 3649(2004).
[16] K.Y. Kim, S.H. Jang, K.H. Shin, H.J. Kim, T. Kang, J.Appl.Phys. **89**, 7612 (2001) **.**
[17] J. F. Bobo, L. Gabillet, M. Bibes, J. Phys.:Condens.Matter **16**, S471(2004)

*Corresponding author: kuncser@infim.ro